2.4. Mutagenicity test

Mutagenicity was determined by the plate incorporation test using *Salmonella* tester strains [3]. Each experiment was carried out on triplicate plates two times with or without the S9 mix, and the mean value was presented as revertants/μg of chemical.

3. Results

3.1. LUMO energy levels and dihedral angles of Nphs

To measure enzymatic reduction, the LUMO energy levels, reduction potential, and orientation of the nitro substituent to the phenanthrene rings

Table 1
LUMO energy levels, reduction potentials, and dihedral angles of NAphs

Chemical	Epc (mV)		LUMO	Dihedral angle
	Epc1	Epc2		
8-N-1-Aph	1042	1631	1429	31.5
6-N-4-Aph	1036	1675	1400	0.1
8-N-4-Aph	1058	1555	1372	32.2
4-N-9-Aph	1120	1662	1326	62.6
5-N-9-Aph	1085	1615	1219	61.7
6-N-9-Aph	1027	1645	1508	0.2
7-N-9-Aph	1004	1664	1436	0.0
5-N-1-APhO	1049	1625	1505	61.0
6-N-1-APhO	972	1572	1663	0.1
8-N-1-APhO	988	1641	1623	33.3
5-N-4-APhO	1214	1619	1427	32.2[a]
6-N-4-APhO	1059	1723	1583	0.7
8-N-4-APhO	1047	1678	1545	31.7
1-N-9-APhO	853	1484	1674	26.5
2-N-9-APhO	964	1628	1696	0.1
3-N-9-APhO	893	1463	1733	0.1
5-N-9-APhO	1029	1568	1494	60.3
1,5-diN-4-APhO	623	1263	2074	30.1[b]
1,8-diN-4-APhO	916	1032	2214	58.2*

[a] and [b]. LUMO energy and dihedral angle were obtained by AM1 calculations based on the structure that was optimized by PM3.
* 8-NO$_2$, 33.5; 1-NO$_2$, 24.7.

were investigated (Table 1). Nitro substituents substituted at the 4 and 5 positions were perpendicular due to the steric effect of the bay region aromatic proton, while those at the 2, 3, 6, and 7 positions were coplanar to the phenanthrene rings (Fig. 1). In contrast, nitro substituents at the 1 and 8 positions had a nitro function with nearly perpendicular orientation to the aromatic ring system because of steric hindrance of the aromatic proton on the peri position, while the calculated dihedral angles varied between 26 and 33˚. This suggested that the orientation of the nitro group generally predicts the mutagenic potency of NAphs. There was no relationship between mutagenicity, reduction potentials and LUMO energy.

3.2. Chemical properties of Nph

Fig. 1 illustrates chemical structures, consisting of Aph derivatives with a nitrogen atom at the 1, 4, and 9 positions, and NAphs, nitrated derivatives, substituted at the 1, 2, 3, 4, 5, 6, 7, and 8 positions in phenanthrene rings and their *N*-oxides.

3.3. Mutagenicity of NAph in Salmonella strains

All NAphs substituted at the 4, 6, 7, and 8 positions were mutagenic for strains TA98 and TA100 without S9 mix while 5-N-9-Aph, 5-N-1-AphO, and 5-N-9-AphO were non-mutagenic or weak mutagens. In NAphO derivatives, 6-N-1-AphO, 8-N-1-AphO, 6-N-4-AphO, and 1, 2, and 3-N-9-AphOs were mutagenic for strains TA98 and TA100, and were direct-acting mutagens, showing activity in the absence of S9 mix while 5-N-1- and 5-N-9-AphOs were non-mutagenic or weakly mutagenic (Table 2). In contrast, mutagenicity for TA98 with S9 mix was assessed, but it was not shown in any NAph derivatives (Table 2). Thus, a mutagenicity test was carried out in the absence of the S9 mix. In these nitrated derivatives, nitro derivatives substituted at the 6 position of phenanthrene rings, 6-N-4-Aph, 6-N-9-Aph, 6-N-1-AphO, and 6-N-4-AphO, showed powerful mutagenicity for strains TA98, TA100, and all YG strains used. Mutagenicity was enhanced by mutant strains producing nitroreductase such as YG1021 and 1026, and those producing *O*-acetyl-
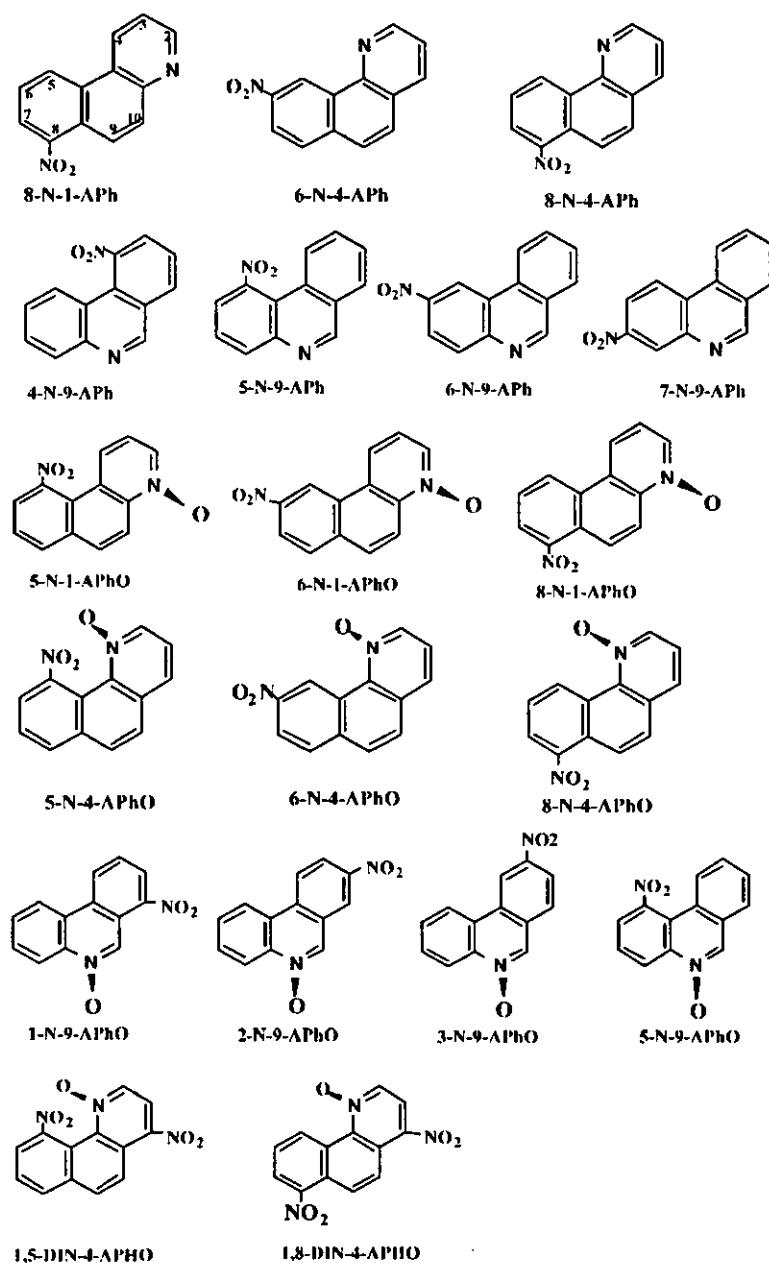
Fig. 1. Chemical structures of NAph's.

transferase such as YG1024 and YG1029. In addition. the nitroreductase activity was also confirmed by the fact that the activity was inhibited by the nitroreductase-deficient strain TA98NR, and similarly, was inhibited by the TA98/1.8-DNP₆. O-acetyltransferase-deficient

strain. Nitro derivatives substituted at the 8 position of the phenanthrene rings such as 8-N-1- and 8-N-4-Aphs. were strongly reverted from autotrophy to prototrophy for strain TA100. These derivatives might arise due to base pair substitution on DNA, showing higher mutageni-

Table 2
Mutagenicity of Naphs

Chemical	Mutagenicity (revertants/µg)								
	TA98 (−S9)	TA98 (+S9)	TA98NR	TA98/1,8DNP6	TA100	YG1021	YG1024	YG1026	YG1029
Spontaneous	29	28	37	11	128	67	86	178	183
8-N-1-Aph	538	8	42	0.3	1046	8479	35600	13040	1246
6-N-4-Aph	2.052	18	149	530	6060	42370	6260	46800	11020
8-N-4-Aph	828		16	141	1528	14480	7980	1282	4018
4-N-9-Aph	112	11	31	48	160	806	609	785	401
5-N-9-Aph	6	ND	2	1.6	7	47	18	53	9
6-N-9-Aph	728	13	168	98	818	1050	3478	5194	788
7-N-9-Aph	452	20	61	185	251	850	1018	918	408
5-N-1-AphO	3	ND	1	0.7	6	16	9	16	8
6-N-1-AphO	150	8	99	82	493	1247	170	5949	718
8-N-1-AphO	38	ND	3	17	113	998	79	1310	122
5-N-4-AphO	63	6	15	19	146	247	87	97	92
6-N-4-AphO	700	17	142	215	1854	6893	1818	7258	4354
8-N-4-AphO	67	ND	4	23	151	1038	786	1528	704
1-N-9-AphO	764	26	170	482	1252	1756	915	4627	897
2-N-9-AphO	213	20	20	36	148	174	639	737	106
3-N-9-AphO	634	11	141	684	173	596	3482	748	413
5-N-9-AphO	4	ND	1	0.5	5	16	12	38	7
1,5-diN-4-AphO	10460	33	6420	1440	2906	24980	11637	9541	6575
1,8-diN-4-AphO	5580	24	5240	8440	8440	21640	11002	48850	5916

ND, not detected.

city in TA100 than TA98. These nitro groups could also be due to steric hindrance of the nitro substituent on the plane of the phenanthrene rings.

Two 1,5- and 1,8-diN-4-AphOs promoted marked mutagenicity for TA98, TA100, and YG strains. Mutagenicity of 1,5- and 1,8-diN-4-AphO corresponded to 166 and 83 times, respectively, that of 5-N-4-AphO and 8-N-4-AphO for TA98, and to 19 and 55 times, respectively, that of 5-N-4- and 8-N-4-AphOs for TA100. Dinitro derivatives substituted at the 1 and 5 positions of the phenanthrene rings were strongly activated by nitroreductase, overproducing mutants more than O-acetyltransferase (Table 2). Both dinitro derivatives, which have relatively lower LUMO energy, showed high mutagenicity for strains TA98 and TA100, and their enzyme rich-mutants. It was found that mutagenicity of 1,5- and 1,8-diN-4-AphO was strongly activated by nitroreductase, rather than O-acetyltransferase, as shown in

YG1021 and 1024, except for reversion for YG 1026 of 1,8-diN-4-AphO.

4. Discussion

We previously reported that the mutagenic potency of Nphs was closely associated with the chemical properties and orientation of nitro substitution of aromatic rings [3]. Nitro substituents at positions 4 and 5 in the phenanthrene rings were perpendicular, while those on positions 2, 3, 6 and 7 were nearly coplanar to the phenanthrene rings (Table 1). It has also been reported that Nphs on positions 1, 8, 9, and 10 were non-coplanar because of steric hindrance of the aromatic proton on the peri position, with dihedral angles varying from 10° to 65° [1,2].

In this study, it was found that NAphs with a nitrogen atom at the 1, 4, and 9 positions of

phenanthrene rings showed potent mutagenicity corresponding to Nphs if they had the same chemical properties as Nphs. Mutagenicity of 4-, 6-, and 7-N-9-Aphs, 1-, 2-, and 3-N-9-AphOs, was potent for *Salmonella* strains, while nitro substituents of 5-N-9-Aph, 5-N-1-AphO, and 5-N-9-AphO were non- or weakly mutagenic. The nitro substituent at the 5 position in the rings was perpendicular on the plane of phenanthrene rings, so mutagenicity was reduced markedly due to steric hindrance. This suggested that the mutagenic potency of these nitro groups closely involved the orientation of nitro substituents of the phenanthrene rings, and the inability to intercalate into the DNA helix.

Nitro substituents on positions 2, 3, 6, and 7 in the phenanthrene rings had a nitro function with coplanar orientation to the parent rings, and had relatively lower LUMO energy levels. In addition, the mutagenicity was markedly enhanced by nitroreductase-overproducing mutants such as YG1021 and YG1026, and by O-acetyltransferase-overproducing mutants such as YG1024 and YG1029. It was considered that these nitro groups were metabolically reduced to nitroso- and amino-derivatives by these enzymes via a hydroxylamino-intermediate.

Two 1,5- and 1,8-diNAphOs were potent mutagens for TA98 and 100, and showed strong reversion from autotrophy to prototrophy by nitroreductase and O-acetyltransferase. Comparing the mutagenic potency of both compounds, 1,8-diNAphO was more strongly activated by nitroreductase than 1,5-diN-4-AphO, e.g. the compound showed 48 850 revertants/μg for YG1026. From the perspective of reduction property, the reduction potentials (mV) of mono- and dinitrophenanthrenes differed; the potentials (Epc1) of mononitrophenanthrenes ranged from −853 to −1214, and those of dinitrophenanthrene (diNph) ranged from −623 to −916 (Table 1). As suggested by Fukuhara et al. [1], nitro substitution causes about a 100–300 mV positive shift in the reduction potentials. Therefore, it was found that the calculated LUMO energy levels were significantly correlated with the first reduction potentials, and the mutagenic potency of NAph was

related to these chemical properties, including LUMO energy and reduction potentials.

With regard to mutagenicity and genotoxicity of nitroazabenzo[*a*]pyrene, we reported that these compounds were potent mutagens for *Salmonella* strains [18], and induced micronuclei in polychromatic erythrocytes in mice and chromosomal aberrations in Chinese hamster lung fibroblast cells [19]. Mutagenicity and genotoxicity of nitroazabenzo[*a*]pyrene N-oxides differed from substitution of nitro function. However, the reduction potentials of 3-nitro-6-azabenzo[*a*]pyrene N-oxide are not markedly different from those of 1-nitro-6-azabenzo[*a*]pyrene N-oxide [18]. In addition, 3,6-dinitrobenzo[*a*]pyrene was much more mutagenic than 1,6-dinitrobenzo[*a*]pyrene. This result indicates that 3,6-dinitrobenzo[*a*]pyrene was readily reduced to stronger nitroso- and amino-derivatives than 1,6-dinitrobenzo[*a*]pyrene [20].

As for a human effect of nitrated aromatic compounds, various chemicals deposited in lung tissues were determined after surgical lung resection; e.g. 1-NP, 1,3-DNP and 3-nitrofluoranthene deposited at higher levels in lung tissues decreased the 5-year survival of patients [21]. It was assumed that increasing amounts of mutagens in lung tissues might promote cell differentiation, with an increase in poor differentiation. As reported previously [3], Nph derivatives were detected in diesel emission particulates, but not from other environmental materials and human lung tissues.

Shmeiser et al. [13,22] demonstrated that aristolochic acid containing Nph carboxylic acids induced multiple tumors in the forestomach, ear duct and small intestine, and urothelial cancer in aristolochic acid nephropathy patients [8]. In addition, DNA adducts of the compound were detected in vitro by incubation of calf thymus DNA and liver homogenate, while tumor initiation by aristolochic acid was associated with carcinogen deoxyadenosine adducts as critical lesions.

We therefore, believe that these mutagens are ubiquitous in the environment, though they have not been detected from environmental materials. It is important that the carcinogenicity of these chemicals be studied in more detail to evaluate

the structure activity relationship of NAphs and their danger to human tissues.

References

[1] K. Fukuhara, N. Miyata, Chemical oxidation of nitrated polycyclic aromatic hydrocarbons: Hydroxylation with superoxide anion radical, Chem. Res. Toxicol. 8 (1995) 27 33.

[2] K. Fukuhara, M. Takei, H. Kageyama, N. Miyata, Di- and trinitrophenanthrenes: synthesis, separation, and reduction property, Chem. Res. Toxicol. 8 (1995) 47 54.

[3] N. Sera, K. Fukuhara, N. Miyata, H. Tokiwa, Mutagenicity of nitrophenanthrene derivatives for *Salmonella typhimurium*: effects of nitroreductase and acetyltransferase, Mutat. Res. 349 (1995) 137 144.

[4] P.P. Fu, Yi.-C. Ni, Y.-M. Zhang, R.H. Heflich, Y.-K. Wang, J.-S. Lai, Effect of the orientation of nitro substituent on the bacterial mutagenicity of nitroben-zo[e]pyrenes, Mutat. Res. 225 (1989) 121 125.

[5] T. Hirayama, T. Watanabe, M. Akita, S. Shimomura, Y. Fujioka, S. Ozasa, S. Fukui, Relationships between structure of nitrated arenes and their mutagenicity in *Salmonella typhimurium*: 2- and 2,7-nitro substituted fluorene, phenanthrene and pyrene, Mutat. Res. 209 (1988) 67 74.

[6] W.A. Vance, D. Levin, Structural features of nitroaro-matics that determine mutagenic activity in *Salmonella typhimurium*, Environ. Mutagen 6 (1984) 797 811.

[7] L. Graeza, P. Ruff, Einfache methods zur bestimmung der aristolochia-sauren durch HPLC, Dtsch. Apoth. Ztg 121 (1981) 2817 2818.

[8] V.M. Arlt, M. Stiborova, H.H. Schmeiser, Aristolochic acid as a probable human cancer hazard in herbal remedies: a review, Mutagenesis 17 (2002) 265 277.

[9] J.M. Pezzuto, S.M. Swanson, W. Mar, C-T. Che, G.A. Cordell, H.H.S. Fong, Evaluation of the mutagenic and cytostatic potential of aristolochic acid (3,4-methylene-dioxy-8-methoxy-10-nitrophenanthrene-1-carboxylic acid) and several of its derivatives, Mutat. Res. 206 (1988) 447 454.

[10] H.H. Schmeiser, B.L. Pool, M. Wiessler, Mutagenicity of the two main components of commercially available carcinogenic aristolochic acid in *Salmonella typhimurium*, Cancer Lett. 23 (1984) 97 101.

[11] U. Mengs, On the histopathogenesis of rat forestomach carcinoma caused by aristolochic acid, Arch. Toxicol. 52 (1983) 209 220.

[12] U. Mengs, W. Lang, J-A. Poch, The Carcinogenic action of aristolochic acid in rats, Arch. Toxicol. 51 (1982) 107 119.

[13] H.H. Schmeiser, J.W.G. Janssen, J. Lyons, H.R. Scherf, W. Pfau, A. Buchmann, C.R. Bartram, M. Wiessler, Aristolochic acid activities *ras* genes in rat tumors at deoxyadenosine residues, Cancer Res. 50 (1990) 5464 5469.

[14] A.K. Debnath, R.L. Lopez de Compadre, A.J. Shuster-man, C. Hansch, Quantitative structure activity relationship investigation of the role of hydrophobicity in regulating mutagenicity in the Ames test: 2. Mutagenicity of aromatic and heteroaromatic nitro compounds in *Salmonella typhimurium* TA100, Environ. Mol. Mutagen 19 (1992) 53 70.

[15] H. Jung, A.U. Shaikh, R.H. Heflich, P.P. Fu, Nitro group orientation, reduction potential, and direct-acting mutagenicity of nitro-polycyclic aromatic hydrocarbons, Environ. Mol. Mutagen. 17 (1991) 169 180.

[16] M.J.S. Dewar, E.W.T. Warford, Electrophile substitution. Part III. The nitration of phenanthrene, J.Am.Chem.Soc. (1956) 3570 3572.

[17] M. Watanabe, M. Ishiodate, T. Nohmi, Sensitive method for the detection of mutagenic nitroarenes and aromatic amines: new derivatives of *Salmonella typhimurium* tester strains possessing elevated *O*-acetyltransferase levels, Mutat. Res. 234 (1990) 337 348.

[18] N. Sera, K. Fukuhara, N. Miyata, K. Horikawa, H. Tokiwa, Mutagenicity of nitroazabenzo[a]pyrene and its related compounds, Mutat. Res. 280 (1992) 81 85.

[19] N. Sera, K. Fukuhara, N. Miyata, H. Tokiwa, Micro-nucleus induction and chromosomal aberration of 1- and 3-nitroazabenzo[a]pyrene and their *N*-oxides, Mutagenesis 16 (2001) 183 187.

[20] H. Tokiwa, N. Sera, A. Nakashima, K. Nakashima, Y. Nakanishi, N. Shigematu, Mutagenic and carcinogenic significance and the possible induction of lung cancer by nitro aromatic hydrocarbons in particulate pollutants, Environ. Health Pers. 102 (1992) 107 110.

[21] H. Tokiwa, N. Sera, Contribution of nitrated polycyclic aromatic hydrocarbons in diesel particles to human lung cancer induction, Polycyclic Aromatic Compounds 21 (2000) 231 245.

[22] H.H. Schmeiser, K.B. Schoepe, M. Wiessler, DNA adduct formation of aristolochic acid I and II in vitro and in vivo, Carcinogenesis 9 (1987) 297 303.

The 4'-hydroxy group is responsible for the in vitro cytogenetic activity of resveratrol

Atsuko Matsuoka [a,*], Kenji Takeshita [b], Ayumi Furuta [c], Masayasu Ozaki [d],
Kiyoshi Fukuhara [e], Naoki Miyata [f]

[a] Division of Medical Devices, National Institute of Health Sciences, 1-18-1 Kamiyoga, Setagaya-ku, Tokyo 158-8501, Japan
[b] The Scientific Analysis Laboratory Inc., Ube-shi, Yamaguchi 755-8633, Japan
[c] Environmental Biological Life Science Research Center Inc., 555 Ukawa, Minakuchi-cho, Koka-gun, Shiga, Japan
[d] Tobacco Science Research Center, Japan Tobacco Inc., 6-2 Umegaoka, Aoba-ku, Kanagawa, Yokohama-city, Kanagawa 227-8512, Japan
[e] Division of Organic Chemistry, National Institute of Health Sciences, 1-18-1 Kamiyoga, Setagaya-ku, Tokyo 158-8501, Japan
[f] Department of Organic and Medicinal Chemistry, Graduate School of Pharmaceutical Sciences, Nagoya City University,
3-1 Tanabe-dori, Mizuho-ku, Nagoya 467-8603, Japan

Received 19 April 2002; received in revised form 30 July 2002; accepted 30 July 2002

Abstract

We previously reported that 3,5,4'-trihydroxy-trans-stilbene (resveratrol), a polyphenolic phytoalexin found in grapes, induces a high frequency of sister chromatid exchanges (SCEs) in vitro. In this study, to investigate structure activity relationships, we synthesized six analogues of resveratrol differing in number and position of hydroxy groups, and we investigated their activity in chromosomal aberration (CA), micronucleus (MN) and sister chromatid exchange (SCE) tests in a Chinese hamster cell line (CHL). Two of the six analogues (3,4'-dihydroxy-trans-stilbene and 4-hydroxy-trans-stilbene) showed clear positive responses in a concentration-dependent manner in all three tests. Both were equal to or stronger than resveratrol in genotoxicity. The 4-hydroxy (OH) analogue had the simplest chemical structure and was the most genotoxic. The other analogues did not have a 4'-hydroxy group. These results suggested that a 4'-hydroxy group is essential to the genotoxicity of stilbenes. © 2002 Elsevier Science B.V. All rights reserved.

Keywords: Resveratrol; The 4'-hydroxy group; Stilbene; Sister chromatid exchanges (SCEs); Chromosome aberrations; Micronuclei

1. Introduction

3,5,4'-Trihydroxy-trans-stilbene (resveratrol) is a polyphenolic phytoalexin found in grapes, peanuts, the Japanese traditional medicine Kojokon, and in other foods. Resveratrol acts as an antioxidant, modulates lipid and lipoprotein metabolism, inhibits platelet aggregation, and has anti-inflammatory, anti-

cancer, and estrogenic activity [1]. Resveratrol may play a role in the inverse correlation between red wine consumption and incidence of cardiovascular disease reported in epidemiological studies (the French paradox). Resveratrol has a similar chemical structure to diethylstilbestrol (DES), which induces numerical chromosome aberrations in vitro [2,3].

We previously reported [4] that resveratrol is negative in the bacterial reverse mutation assay but induces micronuclei (MN) and sister chromatid exchanges (SCEs) in vitro. Having got these results, we became interested in the role of the hydroxy groups on the

* Corresponding author. Tel.: +81-3-3700-9264;
fax: +81-3-3707-6950.
E-mail address: matsuoka@nihs.go.jp (A. Matsuoka).

genotoxic activity. We synthesized six analogues of resveratrol and compared their genotoxic activity with that of resveratrol.

2. Materials and methods

2.1. Cells

The Chinese hamster lung fibroblast cell line (CHL) [5] was maintained in Eagle's minimum essential medium (MEM; GIBCO 61100-061) supplemented with 10% heat-inactivated calf serum (Cansera International Inc., Rexdale, Ont., Canada). The doubling time was around 13 h and the modal chromosome number was 25.

2.2. Chemicals

The chemical structures of 3,5,4′-trihydroxy-*trans*-stilbene (resveratrol; CAS No. 501-36-0) and its six analogues are shown in Fig. 1. Resveratrol was purchased from Sigma (St. Louis, MO, USA). The ana-

logues, 3,5,3′-trihydroxy-*trans*-stilbene (Fig. 1a); 3,5-dihydroxy-*trans*-stilbene (Fig. 1b); 3,4′-dihydroxy-*trans*-stilbene (Fig. 1c); 3,3′-dihydroxy-*trans*-stilbene (Fig. 1d); 3-hydroxy-*trans*-stilbene (Fig. 1e); and 4-hydroxy-*trans*-stilbene (Fig. 1f) were synthesized as previously reported [6]. All the chemicals were dissolved in physiological saline for use.

2.3. Genotoxicity tests

In all experiments we used 10 μg/ml of resveratrol in 48-h treatments as a concurrent positive control and showed the data at the right end of each graph. So we could compare these data with our previous data for resveratrol, and because the molecular weights of resveratrol and its analogues were similar, we used the same concentrations (2.5, 5, 10, and 20 μg/ml) of all the chemicals in all the studies.

2.3.1. Chromosomal aberration (CA) test

Cells were seeded at 1.5×10^5 per plate (60 mm in diameter). After 17-h incubation, they were treated with a test chemical for 24 or 48 h. Colcemid
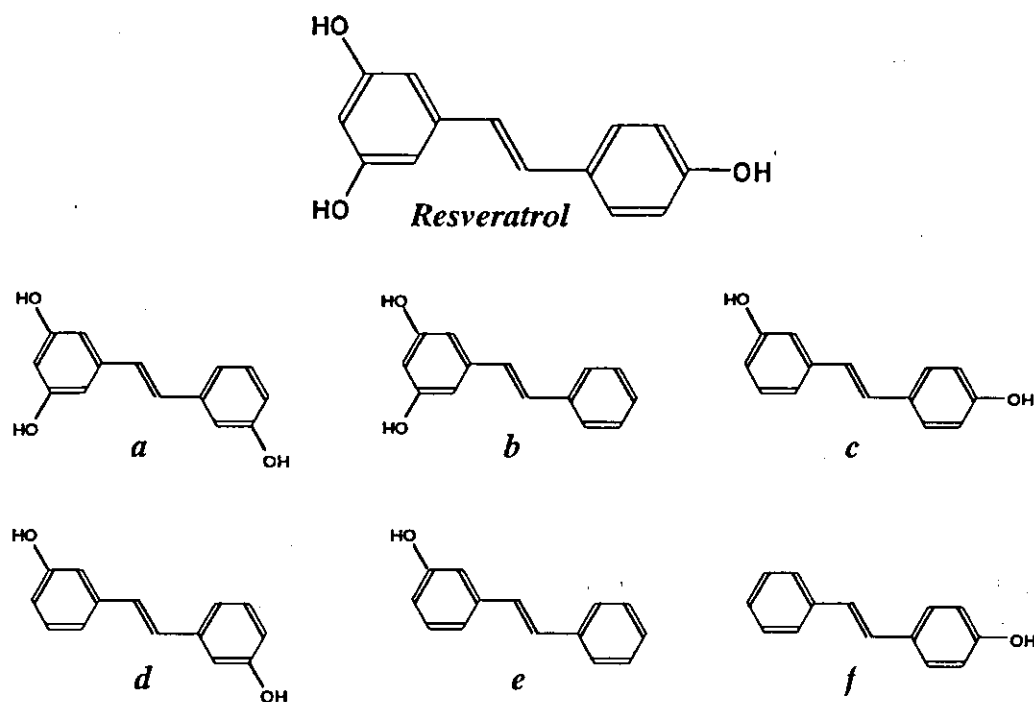
Fig. 1. Chemical structures of resveratrol and its synthesized analogues.

(0.2 μg/ml) was added for the final 2 h. Chromosome preparations were made as previously reported [7] and then stained with Giemsa solution. All slides were coded and the number of cells with numerical and structural aberrations was analyzed for 100 well-spread metaphase cells per concentration. The treatments were judged as negative (−) if the total aberration frequency was < 5.0%, suspect (±) if 5.0 to < 10.0%, and positive (+) if 10.0% or more, based on our historical database [7]. Solvent-treated cells served as the negative control. The CA tests were performed twice.

2.3.2. Micronucleus (MN) test

The MN test was performed twice, in parallel with the CA test. Cells were seeded and treated as they were in the CA test. MN preparations were made as previously reported [8]. The cells were stained by mounting in 40 μg/ml acridine orange in Ca^{2+}–Mg^{2+}-free phosphate-buffered saline and immediately observed at 400× magnification by fluorescence microscopy with a model Olympus BX50 and a U-MWB filter.

All slides were coded and the number of micronucleated cells among 1000 intact interphase cells was scored. In addition, we examined 1000 total cells and scored polynuclear and karyorrhectic (PN) cells and mitotic (M) cells as previously reported [9]. We analyzed the data using a χ^2-test for treated versus control groups. PN and M cell frequencies >100 and 50, respectively, were considered biologically significant.

2.3.3. Sister chromatid exchange (SCE) test

The SCE test was performed in parallel with the CA and MN test. Cells were seeded and treated as they were in the CA test. 5-Bromodeoxyuridine was added to the plate to a final concentration of 5 μM just after addition of the test chemical. Chromosome preparations were made as they were in the CA test. A fluorescence-plus-Giemsa technique [10] was used for sister chromatid differentiation staining as previously reported [11]. SCEs were scored on 25 second-metaphase (M2) cells that had 25 chromosomes and no CAs. Centromeric SCEs were indistinguishable from centric twists and were not scored. Solvent-treated cells served as the negative control. SCE data were analyzed with the Mann–Whitney U-test (the normal, two-tailed version).

3. Results

The results of the CA test are shown in Fig. 2. Significant polyploidy induction was not observed with any analogues (data not shown). Analogues c and f clearly induced structural chromosome aberrations, with peak frequencies of 63% at 10 μg/ml and 65% at 20 μg/ml, respectively. Chromatid breaks and exchanges were the main aberrations for both analogues. Analogue b induced severe cytotoxicity at 20 μg/ml in both the 24- and 48-h treatments. We observed no metaphases when analogue c was administered at 10 or 20 μg/ml for 24 h or 20 μg/ml for 48 h, or when analogue f was administered at 20 μg/ml for 48 h. The frequencies of CAs in cells treated with resveratrol were within expected values.

The results of the MN test are shown in Fig. 3. Reduction of M cell frequency, as shown for analogue c, is a rough indicator of cytotoxicity. Cell number counts performed in parallel showed a similar tendency as the M cell frequency (data not shown).

Analogue c induced a statistically significant increase in MN and PN cell frequency in 48-h treatments at low concentrations, but the frequencies decreased at higher concentrations due to the inhibition of cell division, as shown by the M cell data. Analogue f clearly induced MN and PN cells in a concentration-dependent manner, inducing at the same time, interestingly, gourd-shaped karyorrhectic cells.

The results of the SCE test are shown in Fig. 4. The frequency of SCE in a treatment time with the higher ratio of M2 cells to total cells is represented. Only analogues c and f induced a significant increase in the frequency of SCE with clear concentration response relationships. We observed no metaphases following the administration of analogue c at 10 and 20 μg/ml and analogue f at 20 μg/ml.

4. Discussion

Of the six resveratrol analogues, only analogues c and f were clearly positive in all the cytogenetic studies performed, suggesting that a 4′-hydroxy (OH) group may play a major genotoxic role. Analogues c–e have a three OH group in common, and either another OH at the 4′ or 3′ position or no other OH group. Among those only analogue c induced a strong
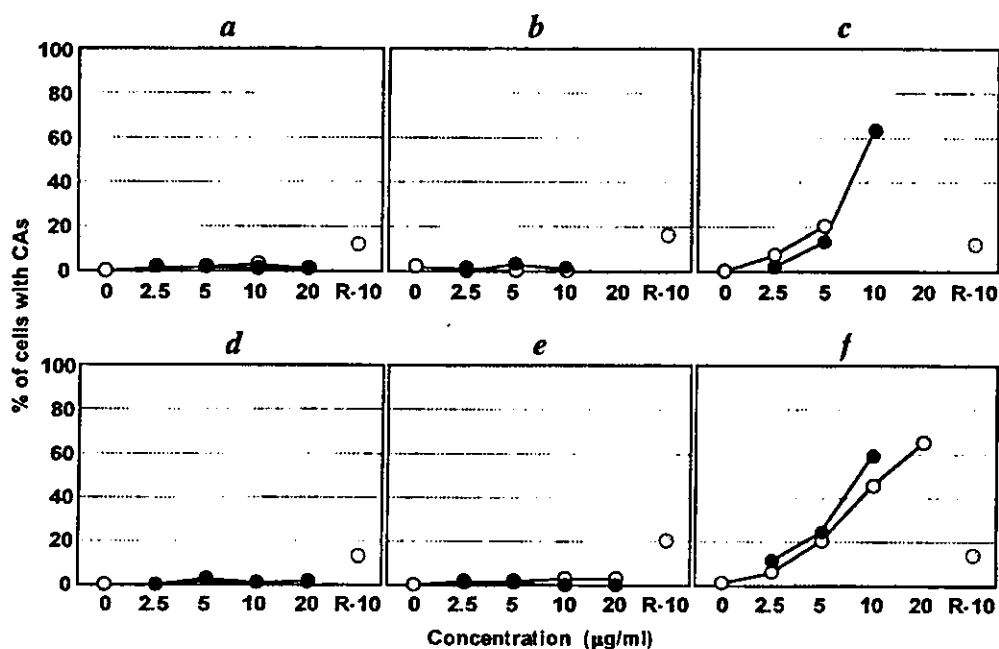
Fig. 2. Chromosome aberrations induced in vitro by resveratrol at 10 μg/ml (R-10) and its analogues. CHL cells were treated for 24 h (O) or 48 h (●).

response, further suggesting the strong contribution of the 4'-OH group. Finally analogue f, which has an OH group only at the 4' position, induced a strong response, indicating directly the genotoxic role of the 4'-OH group.

Although analogues e and f both induced a high frequency of SCEs, analogue f induced a high frequency of PN cells, especially gourd-shaped karyorrhectic cells. That was accompanied by M cell reduction, suggesting induction of a kind of differentiation. It is not clear at present whether these cells remain blocked for a long time or die off.

Two other stilbenes with a 4'-OH group also exert biological activities. One is DES, which is a synthetic estrogen and induces polyploidy at low doses in CHL cells [2,3] and shows a high binding affinity for human ERα and ERβ [12]. The other is tamoxifen, an antiestrogen used to treat breast cancer. The 4-OH metabolite of tamoxifen is a potent antiestrogen [13,14].

Fukuhara et al. [15] reported that resveratrol is a Cu^{2+}-dependent DNA damaging agent whose activity is likely to be due to a copper-peroxide complex. They suggested the binding ability of resveratrol with Cu^{2+} was advantageous to induce Cu^{2+}-dependent

DNA scission. Ahmad et al. also pointed out the significance of DNA damage induced by resveratrol — Cu^{2+} system, which is biologically active as assayed by bacteriophage inactivation [16]. Binding of resveratrol with Cu^{2+} is proved by monitoring the UV absorption spectra, which shows that the absorbance of resveratrol at 305 nm decreases with the concentration of Cu^{2+} [17]. In fact, the same spectral change was observed by analogues e and f whereas the addition of Cu^{2+} did not affect the spectra of the other analogues (data not shown), suggesting the specific binding of Cu^{2+} at the 4'-OH group of stilbene.

We reported that resveratrol shows potent cytogenetic activities previously [4]. In the present study, analogues e and f, which have a OH group at the 4' position that may be responsible for cytogenetic activity of resveratrol, showed strong cytogenetic activities in a concentration-dependent manner in all three tests. In general, genotoxicity tests (the bacterial reverse mutation assay, the CA test, the MN test and so on) have been used to detect gene mutation, chromosome aberration, and DNA damage induced by physical and chemical agents. A positive result in genotoxicity tests has been considered "unbeneficial" to human.
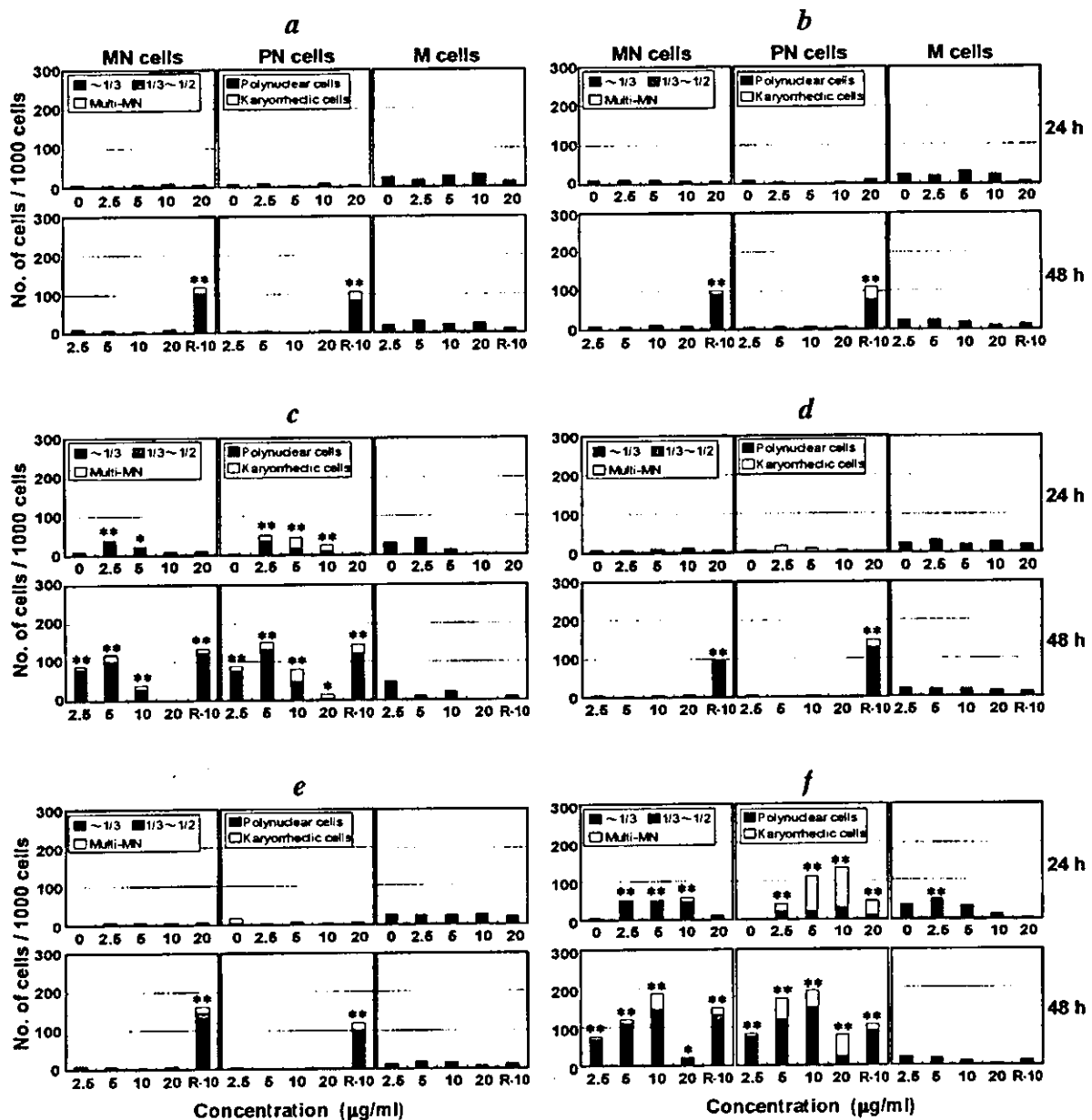
Fig. 3. Micronuclei induced in vitro by resveratrol at 10 μg/ml (R-10) and its analogues: (left) number of MN per 1000 intact interphase cells, black portion: cells with MN whose diameter is less than one-third of the main nucleus diameter, shadowed portion: cells with a MN whose diameter is one-third to one half the diameter of the main nucleus, white portion: cells with multiple MN; (middle) number of PN per 1000 total cells including karyorrhectic cells: black portion: polynuclear cells, white portion: karyorrhectic cells; (right) number of M per 1000 total cells. $^{*}P < 0.05$, $^{**}P < 0.01$.
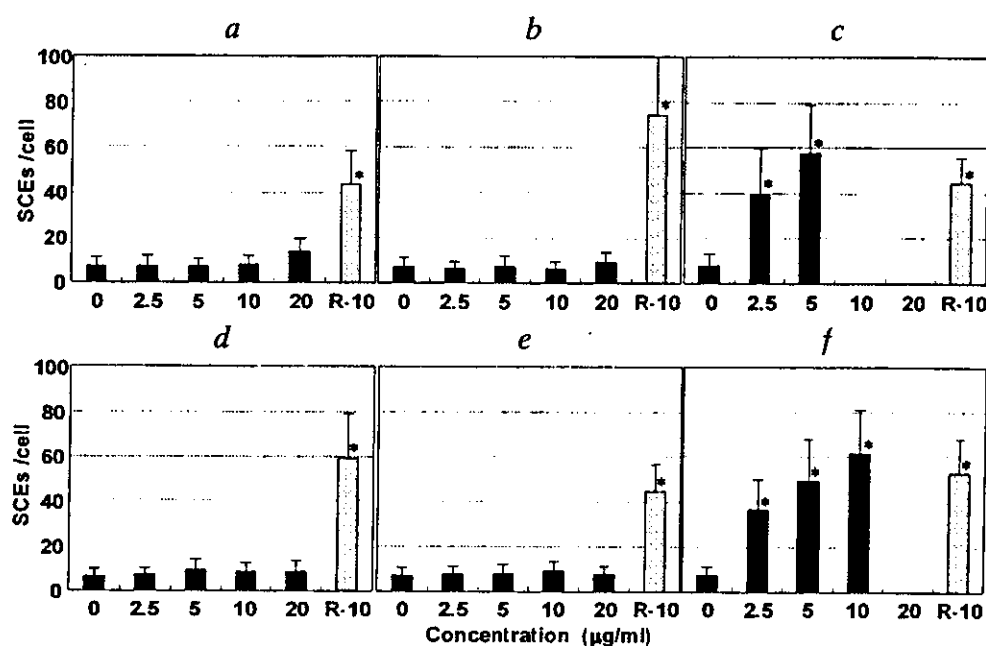
Fig. 4. SCE induced in vitro by resveratrol at 10 µg/ml (R-10) and its analogues. The values indicate the average SCEs per cell of 25 M2 cells and bars indicate S.D. *P < 0.001.

Resveratrol, however, has been reported to show many beneficial effects in pharmacological aspects [1]. Does a negative result in genotoxicity tests mean that the test material is safe and beneficial to human? We think that a negative result might be due to not having any biological activities in a way. We think that a genotoxicity-positive chemical might not always be unbeneficial to human, as shown by resveratrol.

In conclusion, resveratrol, which has a variety of pharmacological activities, induced a high frequency of SCEs. Resveratrol analogues having a 4′-OH group also induced a high frequency of SCE and might also have similar pharmacological effects. Further studies are needed to test that and the role of the 4′-OH group in those effects.

References

[1] L. Fremont, Minireview: biological effects of resveratrol, Life Sci. 66 (2000) 663–673.

[2] M. Sawada, M. Ishidate Jr, Colchicine-like effect of diethylstilbestrol (DES) on mammalian cells in vitro, Mutat. Res. 57 (1978) 175–182.

[3] T. Sofuni (Ed.), Data Book of Chromosomal Aberration Test in Vitro, revised edition 1998, LIC, Tokyo, 1999, p. 184.

[4] A. Matsuoka, A. Furuta, M. Ozaki, K. Fukuhara, N. Miyata, Resveratrol, a naturally occurring polyphenol, induces sister chromatid exchanges in a Chinese hamster lung (CHL) cell line, Mutat. Res. 494 (2001) 107–113.

[5] M. Ishidate Jr, S. Odashima, Chromosome tests with 134 compounds on Chinese hamster cells in vitro—a screening for chemical carcinogens, Mutat. Res. 48 (1977) 337–354.

[6] K. Thakkar, R.L. Geahlen, M. Cushman, Synthesis and protein-tyrosine kinase inhibitory activity of polyhydroxylated stilbene analogues of piceatannol, J. Med. Chem. 36 (1993) 2950–2955.

[7] A. Matsuoka, T. Sofuni, N. Miyata, M. Ishidate Jr, Clastogenicity of 1-nitropyrene, dinitropyrenes, fluorene and mononitrofluorenes in cultured Chinese hamster cells, Mutat. Res. 259 (1991) 103–110.

[8] A. Matsuoka, N. Yamazaki, T. Suzuki, M. Hayashi, T. Sofuni, Evaluation of the micronucleus test using a Chinese hamster cell line as an alternative to the conventional in vitro chromosomal aberration test, Mutat. Res. 272 (1993) 223–236.

[9] A. Matsuoka, K. Matsuura, H. Sakamoto, M. Hayashi, T. Sofuni, A proposal for a simple way to distinguish aneugens from clastogens in the in vitro micronucleus test, Mutagenesis 14 (1999) 385–389.

[10] P. Perry, S. Wolff, New Giemsa method for the differential staining of sister chromatids, Nature 251 (1974) 156–158.

[11] A. Matsuoka, M. Ozaki, K. Takeshita, H. Sakamoto, H.-R. Glatt, M. Hayashi, T. Sofuni, Aneuploidy

induction by benzo[a]pyrene and polyploidy induction by 7,12-dimethylbenz[a]anthracene in Chinese hamster cell lines V79-MZ and V79, Mutagenesis 12 (1997) 365–372.

[12] G.N. Nikov, M. Eshete, R.V. Rajnarayanan, W.L. Alworth, Interactions of synthetic estrogens with human estrogen receptors, J. Endocrinol. 170 (2001) 137–145.

[13] V.C. Jordan, M.M. Collins, L. Rowsby, G. Prestwich, A monohydroxylated metabolite of tamoxifen with potent antiestrogenic activity, J. Endocrinol. 75 (1977) 305–316.

[14] V.C. Jordan, M.E. Lieberman, E. Cormier, R. Koch, J.R. Bagley, P.C. Ruenitz, Structural requirements for the pharmacological activity of nonsteroidal antiestrogens in vitro, Mol. Pharmacol. 26 (1984) 272–278.

[15] K. Fukuhara, N. Miyata, Resveratrol as a new type of DNA-cleaving agent, Bioorg. Med. Chem. Lett. 8 (1998) 3187–3192.

[16] A. Ahmad, S.F. Asad, S. Singh, S.M. Hadi, DNA breakage by resveratrol and Cu(II): reaction mechanism and bacteriophage inactivation, Cancer Lett. 154 (2000) 29–37.

[17] L. Belguendouz, L. Fremont, A. Linard, Resveratrol inhibits metal ion-dependent and independent peroxidation of porcine low-density lipoproteins, Biochem. Pharmacol. 53 (1997) 1347–1355.

Effects of magnesium ion on kinetic stability and spin distribution of phenoxyl radical derived from a vitamin E analogue: mechanistic insight into antioxidative hydrogen-transfer reaction of vitamin E †

Ikuo Nakanishi,*ᵃ Kiyoshi Fukuhara,*ᵇ Tomokazu Shimada,ᵃᶜ Kei Ohkubo,ᵈ Yuko Iizuka,ᵉ Keiko Inami,ᵉ Masataka Mochizuki,ᵉ Shiro Urano,ᵉ Shinobu Itoh,ᶠ Naoki Miyata* and Shunichi Fukuzumi*ᵈ

ᵃ Redox Regulation Research Group, Research Center for Radiation Safety. National Institute of Radiological Sciences, Inage-ku, Chiba 263-8555, Japan. E-mail: nakanis@nirs.go.jp; Fax: +81-43-255-6819; Tel: +81-43-206-3131
ᵇ Division of Organic Chemistry. National Institute of Health Sciences, Setagaya-ku, Tokyo 158-8501, Japan
ᶜ Department of Applied Chemistry. Shibaura Institute of Technology. Minato-ku, Tokyo 108-8548, Japan
ᵈ Department of Material and Life Science, Graduate School of Engineering, Osaka University, CREST, Japan Science and Technology Corporation, Suita, Osaka 565-0871, Japan
ᵉ Division of Organic and Bioorganic Chemistry. Kyoritsu College of Pharmacy. Minato-ku, Tokyo 105-8512, Japan
ᶠ Department of Chemistry. Graduate School of Science, Osaka City University, Sumiyoshi-ku, Osaka 558-8585, Japan
ᵍ Department of Organic and Medicinal Chemistry. Graduate School of Pharmaceutical Sciences. Nagoya City University, Mizuho-ku, Nagoya 467-8603, Japan

The phenoxyl radical **1**˙ of a vitamin E analogue, generated by the reaction of 2,2,5,7,8-pentamethylchroman-6-ol (**III**) with 2,2-di(4-*tert*-octylphenyl)-1-picrylhydrazyl (DPPH˙) or galvinoxyl (G˙), was significantly stabilized by the presence of Mg²⁺. Addition of Mg²⁺ into a solution of **1**˙ resulted in a red shift of the absorption band of **1**˙ as well as a decrease in the *g* value of the EPR spectrum of **1**˙, indicating a complex formation between **1**˙ and Mg²⁺. The complexation between the phenoxyl radical and Mg²⁺ significantly retards the disproportionation reaction of **1**˙ by electronic repulsion between the metal cation and a generated organic cation (**1**⁺), leading to stabilization of the organic radical species. No effect of Mg²⁺ on the rate of hydrogen atom transfer from **III** to DPPH˙ or to G˙ was observed, suggesting that the hydrogen-transfer reaction between **III** and DPPH˙ or G˙ proceeds *via* a one-step hydrogen atom transfer mechanism rather than electron-transfer followed by proton transfer.

Introduction

Vitamin E (α-tocopherol, α-TOH) is a very effective biological antioxidant that can scavenge peroxyl radicals in biological membranes, preventing oxidative injury by toxic and carcinogenic chemicals.[1-3] It has been suggested that α-TOH traps radicals by hydrogen atom transfer from its phenolic OH group to form the corresponding phenoxyl radical species, α-TO˙,[1-3] which readily decomposes, leading to a wide variety of oxidation products of α-tocopherol.[4-21] However, very little is known about the elementary steps of the oxidation reaction of α-TOH. There are two possibilities in the mechanisms of oxidation reactions, *i.e.*, a one-step hydrogen atom transfer or electron transfer followed by proton transfer.[22-24] Svanholm *et al.* have proposed that a first step in the antioxidative activity of tocopherol produces a cation radical by one electron extraction.[25] On the other hand, Burton and Ingold have reported that the

reaction of α-TOH with peroxyls exhibits a substantial deuterium kinetic isotope effect (k_H/k_D 5.4 ± 0.4), indicating that the hydrogen atom transfer is rate controlling.[26] Mukai *et al.* have also demonstrated that the antioxidant activity of tocopherol compounds relates to the total electron-donating character of the alkyl group substituents on the aromatic ring.[27] Thus, it is still not clear whether the hydrogen-transfer reaction of α-TOH proceeds *via* a one-step hydrogen transfer or electron transfer followed by proton transfer. It has been reported that the effect of Mg²⁺ on the hydrogen-transfer rates from NADH (dihydronicotinamide adenine dinucleotide) analogues to aminoxyl or nitrogen radicals provides a reliable criterion for distinguishing between the one-step hydrogen atom transfer and the electron-transfer mechanisms.[28] It has also been demonstrated that metal ions such as Mg²⁺ and Ca²⁺ can stabilize phenoxyl radicals by forming complexes.[29] In this context, the effects of metal ions on the oxidation reaction of α-TOH would be of significant interest to elucidate the mechanistic aspect of the antioxidative reactions of vitamin E.

We report herein that a phenoxyl radical (**1**˙) of a vitamin E analogue, 2,2,5,7,8-pentamethylchroman-6-ol (**III**), generated

in the reaction of III with 2,2-di(4-*tert*-octylphenyl)-1-picryl-hydrazyl (DPPH˙) or galvinoxyl (G˙) is significantly stabilized by interaction with Mg^{2+}. The electronic structure of the Mg^{2+} I˙ complex thus generated has been well characterized by EPR. Detailed spectroscopic and kinetic analyses on the III DPPH˙ (G˙) Mg^{2+} system provide a valuable insight into the mechanism of the hydrogen transfer reactions of a vitamin E analogue to determine whether the reaction between III and DPPH˙ or G˙ proceeds *via* a one-step hydrogen atom transfer or *via* electron transfer.

Experimental

Materials

2,2,5,7,8-Pentamethylchroman-6-ol (III) was purchased from Wako Pure Chemical Ind. Ltd., Japan. 2,2-Bis(4-*tert*-octylphenyl)-1-picrylhydrazyl (DPPH˙) and galvinoxyl (G˙) were obtained commercially from Aldrich. $Mg(ClO_4)_2$ and acetonitrile (MeCN: spectral grade) were purchased from Nacalai Tesque, Inc., Japan and used as received.

Spectral and kinetic measurement

Typically, an aliquot of III (2.0×10^{-2} M) in deaerated MeCN was added to a quartz cuvette (10 mm i.d.) which contained DPPH˙ (1.4×10^{-5} M) in deaerated MeCN (3.0 ml). This led to a hydrogen-transfer reaction from III to DPPH˙. UV VIS spectral changes associated with this reaction were monitored using a Hewlett-Packard 8453 photo diode array spectrophotometer. The rates of hydrogen transfer were determined by monitoring the absorbance change at 543 nm due to DPPH˙ (ε 1.18×10^4 dm^3 mol^{-1} cm^{-1}). Pseudo-first-order or second-order rate constants were determined by a least-squares curve fit using an Apple Macintosh personal computer. The first-order plots of $\ln(A_t A)$ *vs.* time and the second-order plots of $(A A_t)^{-1}$ *vs.* time (A_t and A refer to the final absorbance and the absorbance at the reaction time, respectively) were linear until three or more half-lives with the correlation coefficient $p >$ 0.999. The reaction of III with G˙ was carried out in the same manner and the rates were determined from the absorbance change at 428 nm due to G˙ (ε 1.43×10^5 dm^3 mol^{-1} cm^{-1}).

EPR measurements

Typically, an aliquot of a stock solution of III (1.0×10^{-3} M) was added to a LABOTEC LLC-04B EPR sample tube containing a deaerated MeCN solution of DPPH˙ (1.0×10^{-3} M) in the presence or absence of 0.1 M $Mg(ClO_4)_2$ under an atmospheric pressure of Ar. EPR spectra of the phenoxyl radical I˙ produced in the reaction between III and DPPH˙ were taken on a JEOL X-band spectrometer (JES-FA100). The EPR spectra were recorded under nonsaturating microwave power conditions. The magnitude of modulation was chosen to optimize the resolution and the signal-to-noise (S/N) ratio of the observed spectra. The g values and the hyperfine coupling constants were calibrated with a Mn^{2+} marker. Computer simulation of the EPR spectra was carried out using Calleo ESR Version 1.2 program (Calleo Scientific Publisher) on an Apple Macintosh personal computer.

Cyclic voltammetry

The cyclic voltammetry measurements were performed on a BAS 100 W electrochemical analyzer in deaerated MeCN containing 0.10 M NBu_4ClO_4 as a supporting electrolyte. The Pt working electrode (BAS) was polished with BAS polishing alumina suspension and rinsed with acetone before use. The counter electrode was a platinum wire. The measured potentials were recorded with respect to an Ag/AgNO₃ (0.01 M) reference electrode. The $E_{1/2}$ values (*vs.* Ag/AgNO₃) were converted to

those *vs.* SCE by adding 0.29 V.[30] All electrochemical measurements were carried out at 298 K under an atmospheric pressure of argon.

Theoretical calculations

Density functional calculations were performed on a COMPAQ DS20E computer using the Amsterdam Density Functional (ADF) program version 1999.02 developed by Baerends *et al.*[31] The electronic configurations of the molecular systems were described by an uncontracted triple-ζ Slater-type orbital basis set (ADF basis set IV) with a single polarization function used for each atom. Core orbitals were frozen through 1s (C, O) and 2p (Mg). The calculations were performed using the local exchange-correlation potential by Vosko *et al.*[32] and the non-local gradient corrections by Becke[33] and Perdew[34] during the geometry optimizations. First-order scalar relativistic corrections were added to the total energy. Final geometries and energetics were optimized by using the algorithm of Versluis and Ziegler[35] provided in the ADF package and were considered converged when the changes in bond lengths between subsequent iterations fell below 0.01 A.

Results and discussion

Stabilization of phenoxyl radical of a vitamin E analogue by magnesium ion

When III was added to a deaerated acetonitrile (MeCN) solution of DPPH˙, the visible absorption band at 543 nm due to DPPH˙ immediately decreased, accompanied by an increase in the absorption bands at 402 and 423 nm with clear isosbestic points at 343, 374, and 437 nm as shown in Fig. 1. The absorp-
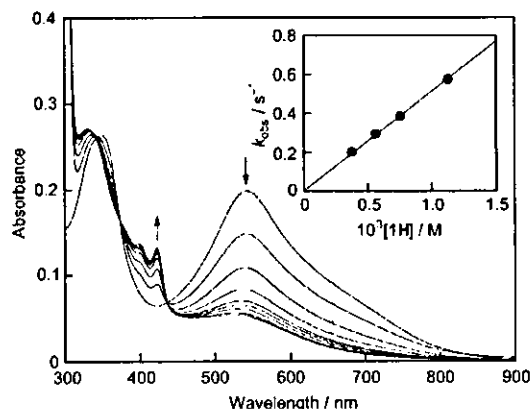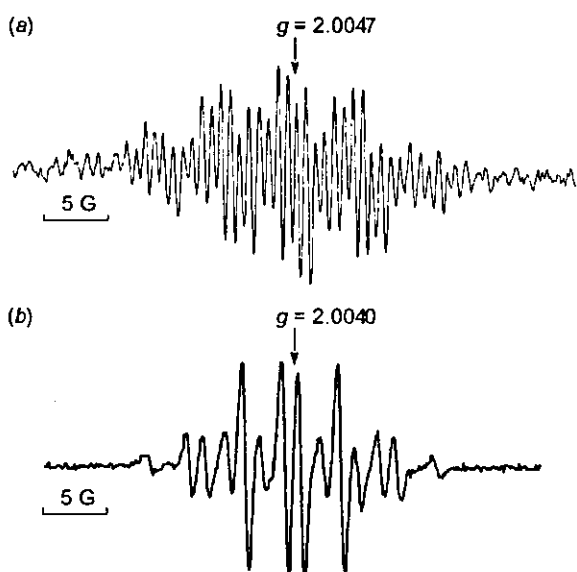

Fig. 1 Spectral changes in the reaction of III (7.5×10^{-5} M) with DPPH˙ (1.4×10^{-5} M) in deaerated MeCN at 298 K (2 s intervals). Inset: Plot of k_{obs} *vs.* [III].

tion bands around 400 nm and the broad band around 530 nm are typical for phenoxyl radical species of α-tocopherol.[36] This indicates that hydrogen atom transfer from III to DPPH˙ occurs to produce the corresponding phenoxyl radical I˙ and DPPH₂ [eqn. (1)]. In fact, the EPR spectrum having a g value of 2.0047 due to I˙ was observed in the reaction of III with DPPH˙ in deaerated MeCN at 298 K as shown in Fig. 2(a). The EPR signal of I˙ gradually decreased with prolonged reaction time.[37] The observed hyperfine structure in Fig. 2(a) is well reproduced by the computer simulation with the hyperfine splitting (hfs) values of one set of methylene protons (1.39 G) and three sets of methyl protons (5.87, 4.40 and 0.86 G). Based on the reported hfs values for I˙ in benzene[37d] as well as the calculated spin density of I˙ by the Amsterdam Density Functional (ADF) method (see Experimental section), we assigned those hfs values as shown in Table 1.

Radical	g	a(3H')	a(3H')	a(3H')	a(2H')
1˙	2.0047	5.87	4.40	0.86	1.39
1˙'	2.0476 '	6.04 '	4.55 '	0.96 '	1.48 '
Mg²⁺-1˙	2.0040	3.35		4.86	

' Taken from ref 37d (in benzene).

Fig. 2 (a) EPR spectrum of 1˙ generated in the reaction of 1H (1.0 × 10⁻⁴ M) with DPPH' (1.0 × 10⁻⁴ M) in deaerated MeCN at 298 K; (b) EPR spectrum of the Mg²⁺-1˙ complex generated in the reaction of 1H (1.0 × 10⁻⁴ M) with DPPH' (1.0 × 10⁻⁴ M) in the presence of 0.1 M Mg(ClO₄)₂ in deaerated MeCN at 298 K.
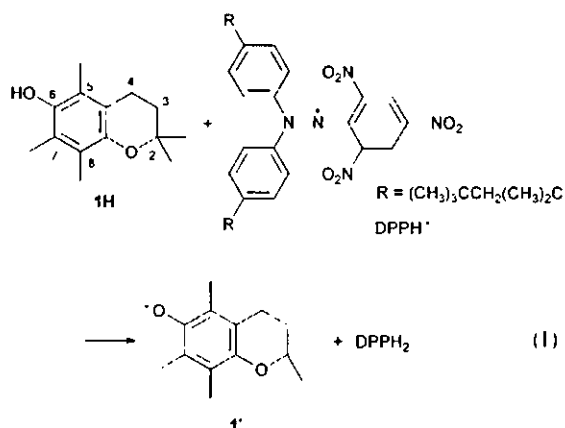
The decrease in the absorbance at 543 nm due to DPPH' obeyed pseudo-first-order kinetics under conditions where the concentration of 1H was maintained at more than a 10-fold excess of DPPH' concentration. The pseudo-first-order rate constant (k_obs) increases linearly with an increase in concentration of 1H as shown in the inset of Fig. 1. From the slope of the linear plot of k_obs vs. [1H] the second-order rate constant for hydrogen transfer (k_HT) from 1H to DPPH' was obtained as 5.1 × 10² M⁻¹ s⁻¹. This value is nearly the same as the k_HT value (4.9 × 10² M⁻¹ s⁻¹) reported for hydrogen transfer from α-tocopherol to DPPH' in MeCN.³⁸ When DPPH' was replaced by the galvinoxyl radical (G˙), the decay of the absorption band at 428 nm due to G˙ was observed upon addition of 1H to a deaerated MeCN solution of G˙. Such spectral change can be

ascribed to a hydrogen atom transfer from 1H to G˙ [eqn. (2)]. The rate constant for hydrogen transfer from 1H to G˙ was determined in the same manner as in the case of DPPH' as 3.0 × 10³ M⁻¹ s⁻¹, which is about 6-fold larger than that determined for DPPH'. Although the absorption bands at 402 and 423 nm due to 1˙ generated by hydrogen transfer from 1H to G˙ could not be observed because of the overlap with the large absorption band at 428 nm due to G˙, the formation of 1˙ can be confirmed from its EPR spectrum.


1H + [structure] ⟶ 1˙ + GH   (2)

G˙
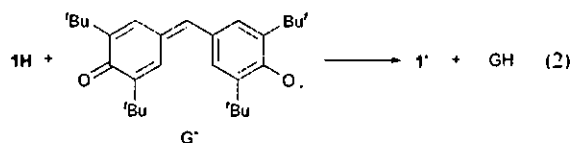
The phenoxyl radical (1˙) generated by hydrogen transfer from 1H to DPPH' gradually decomposed at room temperature (Fig. 3(a)).³⁶ The decrease in the absorption band at 423 nm due
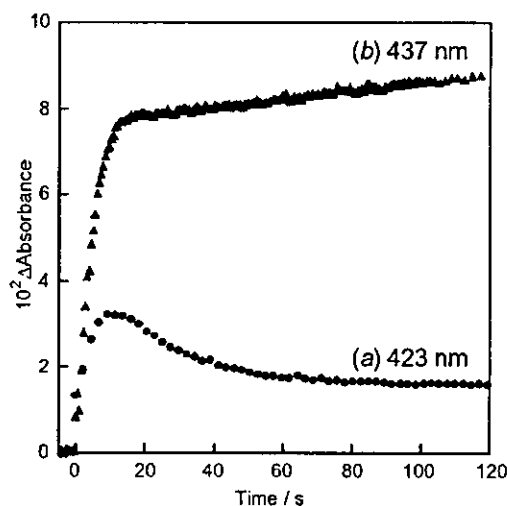
Fig. 3 (a) Time course of the absorption change at 423 nm due to 1˙ (black circles) in the reaction of 1H (7.5 × 10⁻⁴ M) with DPPH' (1.4 × 10⁻³ M) in deaerated MeCN at 298 K (b) Time course of the absorption change at 437 nm due to the Mg²⁺-1˙ complex (black triangles) in the reaction of 1H (7.5 × 10⁻⁴ M) with DPPH' (1.4 × 10⁻³ M) in the presence of 0.1 M Mg(ClO₄)₂ in deaerated MeCN at 298 K

to 1˙ obeys second-order kinetics in agreement with the decay occurring via a bimolecular disproportionation reaction to give 1H and the corresponding quinone methide (2) as shown in Scheme 1.²⁹,³⁶ The second-order rate constant (k_dec) for
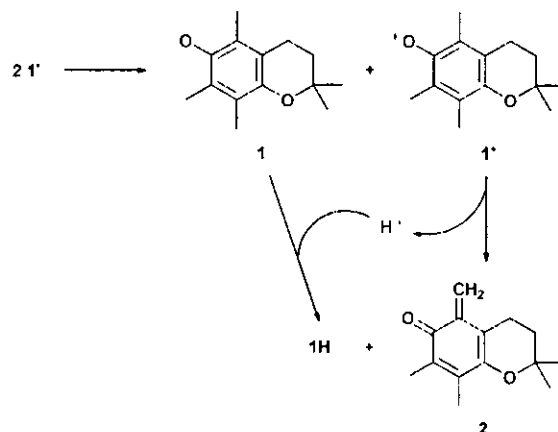
Scheme 1

the decomposition of I' in deaerated MeCN at 298 K was determined from the second-order plot as 2.7×10^3 M^{-1} s^{-1}.[39]

In the presence of Mg(ClO$_4$)$_2$ (0.1 M), the reaction between III and DPPH' also took place to give the phenoxyl radical species in deaerated MeCN, the absorption bands of which, however, were shifted from 402 and 423 nm to 412 and 437 nm, respectively. It should be noted that no decay of these absorption bands was observed, demonstrating significantly the enhanced stability of the phenoxyl radical species in the presence of Mg(ClO$_4$)$_2$ (Fig. 3(b)). Since the disproportionation reaction between the two molecules of I' involves both oxidation and reduction, I' must act as both the oxidant and reductant (Scheme 1).[29] Although the complexation of the Lewis acid such as Mg^{2+} with I' would accelerate the reduction of I' to the phenolate I , it would decelerate the oxidation process due to the repulsive interaction between the oxidized product I' and Mg^{2+} at the same time.[29] Thus, the destabilization of I' by Mg^{2+} governs the overall reactivity in the disproportionation reaction to stabilize the phenoxyl radical species I' in the presence of Mg^{2+}.

Effects of magnesium ion on the spin distribution of the phenoxyl radical

The EPR spectrum of the Mg^{2+} complex of I' generated in the reaction of III with DPPH' in the presence of 0.1 M Mg(ClO$_4$)$_2$ in deaerated MeCN is observed as shown in Fig. 2(b). The g value of the EPR spectrum of Mg^{2+} I' is determined as 2.0040, which is appreciably smaller than the g value of I' (2.0047). The smaller g value of Mg^{2+} I' (2.0040) than that of I' (2.0047) indicates that the spin density on oxygen nuclei in Mg^{2+} I' is decreased by complexation with Mg^{2+}.[29] The hyperfine structure can be reproduced by computer simulation with the hyperfine splitting (hfs) values of two sets of methyl protons (4.86 and 3.35 G). As in the case of I', we assigned those hfs values as shown in Table 1 based on the calculated spin density of Mg^{2+} I' by the ADF method (see Experimental section).

It is interesting to note that the spin density at C(8) of Mg^{2+} I' (ρ 0.094) calculated using the ADF method is larger than that at C(5) (ρ 0.038) (see Supplementary Fig. S(1b)†), while a relatively large amount of the spin density is accumulated at the C(5) and C(7) positions in I' (Fig. S(1a)). The same EPR spectrum of Mg^{2+} I' was obtained for the III G' Mg^{2+} system. No interaction between Mg^{2+} and DPPH' or G' has been detected in the electronic spectra as well as in the g values and hyperfine splitting constants of the EPR spectra of DPPH' or G' in the presence of Mg^{2+}. No change in the absorption spectra was observed either upon addition of Mg^{2+} to III.

Effects of magnesium ion on the rate of hydrogen transfer

No effect of Mg^{2+} on the k_{HT} values of the hydrogen-transfer reaction of III was observed in the case of DPPH' or G' used as a hydrogen abstracting agent (see Supplementary Fig. S(2)†). Thus, there may be no contribution of electron transfer from III to DPPH' or G' in the hydrogen-transfer reaction, which may thereby proceed via a one-step hydrogen-transfer process.[28] If the hydrogen transfer from III to DPPH' or G' involves an electron-transfer process as the rate-determining step, the rate of hydrogen transfer would be accelerated by the presence of Mg^{2+} which is known to accelerate the electron transfer to DPPH' and G'.[28]

Judging from the one-electron oxidation potential of III (E^0_{ox} vs. SCE 0.77 V) which is higher than the one-electron reduction potential of DPPH' (E^0_{red} vs. SCE 0.18 V) or G' (E^0_{red} vs. SCE 0.05 V), the free energy change of electron transfer from III to DPPH' or G' is positive [ΔG^0_{el}(in eV) $= e(E^0_{\text{ox}} - E^0_{\text{red}}) > 0$, where e is the elementary charge], and thereby the electron-transfer step is endergonic. In such a case, the overall rate of hydrogen transfer (k_{HT}) which consists of
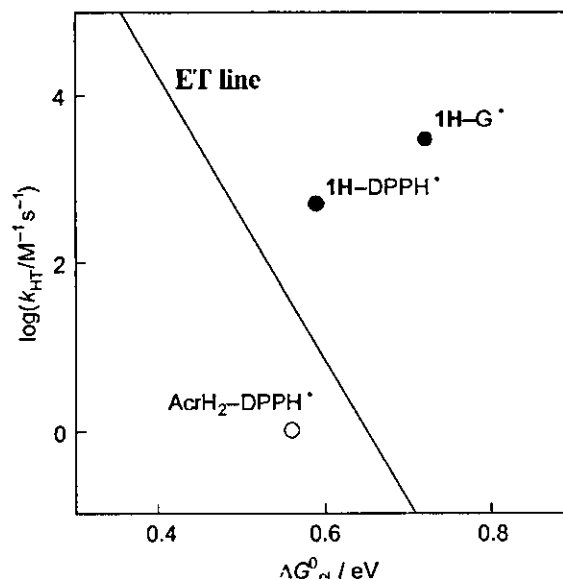

Fig. 4 Plot of the rate constant of hydrogen transfer from III or AcrH$_2$ to DPPH' or G' (logk_{HT}) vs. the free energy of electron transfer from III or AcrH$_2$ to DPPH' or G' (ΔG^0_{el}). The solid line shows the dependence of the calculated rate constant of electron transfer (k_{el}) on ΔG^0_{el} based on eqn. (3), see text.

electron-transfer and proton-transfer steps would be slower than the initial electron-transfer rate (k_{el}). The maximum k_{el} value is evaluated from the ΔG^0_{el} value by eqn. (3), where Z is the frequency factor taken as 1×10^{11} M^{-1} s^{-1}.[*] and k_{B} is the Boltzmann constant.

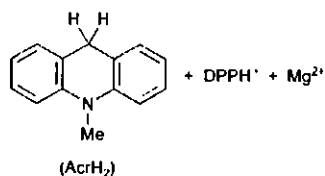$$k_{\text{el}} = Z\exp(-\Delta G^0_{\text{el}}/k_{\text{B}}T) \qquad (3)$$

Fig. 4 shows a plot of log k_{HT} versus ΔG^0_{el} calculated by eqn. (3) (denoted by the ET line). The k_{HT} values of both the III DPPH' and III G' systems (black circles) are significantly above the ET line. The k_{HT} value of the III DPPH' system as well as that of the III G' system, which is much larger than the corresponding k_{el} value, indicates that the hydrogen transfer proceeds via a direct one-step hydrogen transfer rather than via electron transfer. In such a case, no effect of Mg^{2+} on the k_{HT} values should be observed, as is confirmed experimentally.

On the other hand, the hydrogen transfer from an NADH analogue, 10-methyl-9,10-dihydroacridine (AcrH$_2$) (E^0_{ox} 0.81 V vs. SCE)[41] to DPPH' has been reported to proceed via electron transfer from AcrH$_2$ to DPPH', which is accelerated by the presence of Mg^{2+}, followed by proton transfer from AcrH$_2^{\cdot+}$ to DPPH to yield the acridinyl radical (AcrH') and DPPH$_2$.[28] The resulting AcrH' is a much stronger reductant than AcrH$_2$, judging from the negative oxidation potential (E^0_{ox} 0.43 V)[28] as compared to that of AcrH$_2$ (0.81 V),[41] and thereby AcrH' can readily transfer an electron to another DPPH' molecule to yield AcrH$^+$ (Scheme 2).[28] In such a case, the k_{HT} value (white circle in Fig. 4), which is much smaller than the corresponding maximum k_{el} value, indicates that the hydrogen transfer proceeds via electron transfer followed by proton transfer.
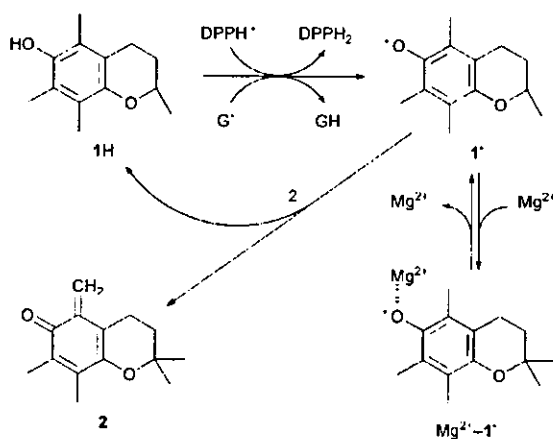
In conclusion, the phenoxyl radical of the vitamin E analogue III generated by hydrogen atom transfer from III to DPPH' or G' is significantly stabilized by Mg^{2+} by complexation of I' with Mg^{2+} as shown in Scheme 3.

No effect of Mg^{2+} on the hydrogen transfer rate from III to DPPH' or G' indicates that the hydrogen-transfer reaction from III to DPPH' or G' proceeds via a one-step hydrogen-transfer process rather than via electron transfer.

H H

+ DPPH˙ + Mg²⁺

Me

(AcrH₂)

[AcrH₂˙⁺ DPPH⁻–Mg²⁺]

DPPH₂ + Mg²⁺

AcrH˙ ——→ AcrH⁺

DPPH˙ + H˙   DPPH₂

Scheme 2

HO

DPPH˙   DPPH₂

G˙   GH

1H

˙O

1˙

2

Mg²⁺   Mg²⁺

CH₂

O

Mg²⁺

˙O

2

Mg²⁺–1˙

Scheme 3

Acknowledgements

References

1 L. J. Machlin, in *Hand Book of Vitamins*, ed. L. J. Machlin, Marchel Dekker, New York, 2nd edn., 1991, pp. 99–144.
2 C. K. Chow, *Free Radical Biol. Med.*, 1991, 11, 215.
3 G. W. Burton and K. U. Ingold, *Acc. Chem. Res.*, 1986, 19, 194.
4 C. Suarna, D. C. Craig, K. J. Cross and P. T. Southwell-Keely, *J. Org. Chem.*, 1988, 53, 1281.
5 M. Matsuo, S. Matsumoto and T. Ozawa, *Org. Magn. Reson.*, 1983, 21, 261.
6 T. Doba, G. W. Burton and K. U. Ingold, *J. Am. Chem. Soc.*, 1983, 105, 6505.
7 G. W. Burton, T. Doba, E. Gabe, L. Hughes, F. L. Lee, L. Prasad and K. U. Ingold, *J. Am. Chem. Soc.*, 1985, 107, 7053.
8 S. Urano, S. Yamanoi, Y. Hattori and M. Matsuo, *Lipids*, 1977, 12, 105.

9 W. A. Skinner and P. Alaupovic, *J. Org. Chem.*, 1963, 28, 2854.
10 H. Meerwein, *Angew. Chem.*, 1955, 67, 374.
11 K. Dimroth, W. Umbach and H. Thomas, *Chem. Ber.*, 1967, 100, 132.
12 P. D. Boyer, *J. Am. Chem. Soc.*, 1951, 73, 733.
13 W. Durckheimer and L. A. Cohen, *J. Am. Chem. Soc.*, 1964, 86, 4388.
14 C. Martius and H. Eilingsfeld, *Liebigs Ann. Chem.*, 1957, 607, 159.
15 W. John, E. Dietzel and W. Emte, *Z. Physiol. Chem.*, 1939, 257, 173.
16 W. A. Skinner and R. M. Parkhurst, *J. Org. Chem.*, 1966, 31, 1248.
17 J. L. G. Nilsson, J. O. Branstad and H. Sievertsson, *Acta Pharm. Suec.*, 1968, 5, 509.
18 D. R. Nelan and C. D. Robeson, *J. Am. Chem. Soc.*, 1962, 84, 2963.
19 M. Jujimaki, K. Kanamaru, T. Kurata and O. Igarashi, *Agric. Biol. Chem.*, 1970, 34, 1781.
20 V. L. Frampton, W. A. Skinner, P. Cambour and P. S. Bailey, *J. Am. Chem. Soc.*, 1960, 82, 4632.
21 E. M. Dean, K. B. Hindley, L. E. Houghton and M. L. Robinson, *J. Chem. Soc., Perkin Trans. 1*, 1976, 600.
22 S. Fukuzumi, in *Advances in Electron Transfer Chemistry*, ed. P. S. Mariano, JAI Press, Greenwich, 1992, vol. 2, pp. 67–175; and refs. cited therein.
23 (a) D. Mauzerall and F. H. Westheimer, *J. Am. Chem. Soc.*, 1955, 77, 2261; (b) R. H. Abeles, R. F. Hutton and F. H. Westheimer, *J. Am. Chem. Soc.*, 1957, 79, 712.
24 (a) E. M. Kosower, in *Free Radicals in Biology*, ed. W. A. Pryor, Academic Press, New York, 1976, vol. II, ch. 1; (b) S. Fukuzumi and T. Tanaka, in *Photoinduced Electron Transfer*, ed. M. A. Fox and M. Chanon, Elsevier, Amsterdam, 1988, Part C, ch. 10.
25 U. Svanholm, K. Bachgaard and V. Parker, *J. Am. Chem. Soc.*, 1974, 96, 2409.
26 G. W. Burton, T. Doba, E. J. Gabe, L. Hughes, F. L. Lee, L. Prasad and K. U. Ingold, *J. Am. Chem. Soc.*, 1985, 107, 7053.
27 (a) K. Mukai, K. Fukuda, K. Tajima and K. Ishizu, *J. Org. Chem.*, 1988, 53, 430; (b) K. Mukai, Y. Kageyama, T. Ishida and K. Fukuda, *J. Org. Chem.*, 1989, 54, 552.
28 S. Fukuzumi, Y. Tokuda, Y. Chiba, L. Greci, P. Carloni and E. Damiani, *J. Chem. Soc., Chem. Commun.*, 1993, 1575.
29 S. Itoh, H. Kumei, S. Nagatomo, T. Kitagawa and S. Fukuzumi, *J. Am. Chem. Soc.*, 2001, 123, 2165.
30 K. Mann and K. K. Barnes, in *Electrochemical Reactions in Nonaqueous Systems*, Marcel Dekker Inc., New York, 1990.
31 (a) E. J. Baerends, D. E. Ellis and P. Ros, *Chem. Phys.*, 1973, 2, 41; (b) G. te Velde and E. J. Baerends, *J. Comput. Phys.*, 1992, 99, 84.
32 S. H. Vosko, L. Wilk and M. Nusair, *Can. J. Phys.*, 1980, 58, 1200.
33 A. Becke, *Phys. Rev. A*, 1988, 38, 3098.
34 (a) J. P. Perdew, *Phys. Rev. B*, 1986, 33, 8822; (b) J. P. Perdew, *Phys. Rev. B*, 1986, 34, 7406.
35 L. Versluis and T. Ziegler, *J. Chem. Phys.*, 1988, 88, 322.
36 V. W. Bowry and K. U. Ingold, *J. Org. Chem.*, 1995, 60, 5456.
37 For the EPR spectrum of the phenoxyl radical derived from α-tocopherol and its analogues, see (a) R. J. Singh, S. P. A. Goss, J. Joseph and B. Kalyanaraman, *Proc. Natl. Acad. Sci. USA*, 1998, 95, 12912; (b) B. Kalyanaraman, V. M. Darley-Usmar, J. Wood, J. Joseph and S. Parthasarathy, *J. Biol. Chem.*, 1992, 267, 6789; (c) B. Kalyanaraman, W. E. Antholine and S. Parthasarathy, *Biochim. Biophys. Acta*, 1990, 1035, 286; (d) G. W. Burton, T. Doba, E. J. Gabe, L. Hughes, F. L. Lee, L. Prasad and K. U. Ingold, *J. Am. Chem. Soc.*, 1985, 107, 7053; (e) J. Tsuchiya, E. Niki and Y. Kamiya, *Bull. Chem. Soc. Jpn.*, 1983, 56, 229; (f) W. Boguth and H. Niemann, *Biochim. Biophys. Acta*, 1971, 248, 121.
38 L. Valgimigli, J. T. Banks, K. U. Ingold and J. Lusztyk, *J. Am. Chem. Soc.*, 1995, 117, 9966.
39 The second-order decomposition rate constant for α-TO˙ in chlorobenzene at 296 K is reported as 3.9 × 10³ M⁻¹ s⁻¹. See ref. 36 and refs cited therein.
40 (a) R. A. Marcus, *Annu. Rev. Phys. Chem.*, 1964, 15, 155; (b) R. A. Marcus, *Angew. Chem., Int. Ed. Engl.*, 1993, 32, 1111.
41 S. Fukuzumi, Y. Tokuda, T. Kitano, T. Okamoto and J. Otera, *J. Am. Chem. Soc.*, 1993, 115, 8960.

Effects of Metal Ions Distinguishing between One-Step Hydrogen- and Electron-Transfer Mechanisms for the Radical-Scavenging Reaction of (+)-Catechin

Ikuo Nakanishi,*,† Kentaro Miyazaki,‡,§ Tomokazu Shimada,‡,§ Kei Ohkubo,¹ Shiro Urano,§
Nobuo Ikota,† Toshihiko Ozawa,† Shunichi Fukuzumi,*,¹ and Kiyoshi Fukuhara*,‡

*Redox Regulation Research Group, Research Center for Radiation Safety,
National Institute of Radiological Sciences, Inage-ku, Chiba 263-8555, Japan, Division of Organic Chemistry,
National Institute of Health Sciences, Setagaya-ku, Tokyo 158-8501, Japan, Department of Applied Chemistry,
Shibaura Institute of Technology, Minato-ku, Tokyo 108-8548, Japan, Department of Material and Life Science,
Graduate School of Engineering, Osaka University, CREST, Japan Science and Technology Corporation (JST),
Suita, Osaka 565-0871, Japan*

A kinetic study of a hydrogen-transfer reaction from (+)-catechin (1) to galvinoxyl radical (G•) has been performed using UV–vis spectroscopy in the presence of $Mg(ClO_4)_2$ in deaerated acetonitrile (MeCN). The rate constants of hydrogen transfer from 1 to G• determined from the decay of the absorbance at 428 nm due to G• increase significantly with an increase in the concentration of Mg^{2+}. The kinetics of hydrogen transfer from 1 to cumylperoxyl radical has also been examined in propionitrile (EtCN) at low temperature with use of ESR. The decay rate of cumylperoxyl radical in the presence of 1 was also accelerated by the presence of scandium triflate [$Sc(OTf)_3$ ($OTf = OSO_2CF_3$)]. These results indicate that the hydrogen-transfer reaction of (+)-catechin proceeds via electron transfer from 1 to oxyl radicals followed by proton transfer rather than via a one-step hydrogen atom transfer. The coordination of metal ions to the one-electron reduced anions may stabilize the product, resulting in the acceleration of electron transfer.

Introduction

Catechins contained in green tea are a class of bioflavonoids that show significant antioxidative activity.[1–9] It has been suggested that catechins trap radical species by hydrogen atom transfer from its phenolic OH group on the B ring.[10,11] However, little is known about the elementary steps of hydrogen-transfer reactions from catechins to radical species. There are two possibilities in the mechanism of hydrogen-transfer reactions from phenolic antioxidants to radical species, i.e., a one-step hydrogen atom transfer or electron transfer followed by proton transfer.[12] Kusu et al. have recently reported the quantitative relationship between the antioxidative activity of catechins and their oxidation potentials determined by flow-through column electrolysis.[13] The galloylated catechins having more negative oxidation potentials than those of nongalloylated catechins show more efficient antioxidative activity on NADPH-dependent microsomal lipid peroxidation than the nongalloylated catechins.[13] On the other hand, based on the gas-phase bond dissociation enthalpy and ionization potential calculated by density functional method, Wright et al. have concluded that in most hydrogen-transfer reactions of phenolic antioxidants, hydrogen-atom transfer will be dominant rather than electron transfer.[12] Thus, it is still not clear whether the hydrogen-transfer reaction of catechins proceeds via a one-step hydrogen atom transfer or electron transfer followed by proton transfer. It has

previously been demonstrated that the effect of Mg^{2+} on the hydrogen-transfer rates from NADH (dihydronicotinamide adenine dinucleotide) analogues to aminoxyl or nitrogen radicals provides a reliable criterion for distinguishing between the one-step hydrogen atom transfer and the electron-transfer mechanisms.[14]

We report herein the effect of metal ions, such as Mg^{2+} and Sc^{3+}, on the rates of hydrogen transfer from (+)-catechin (1) to oxyl radical species, such as galvinoxyl and cumylperoxyl radicals. Cumylperoxyl radical, which is much less reactive than alkoxyl radicals, is known to follow the same pattern of relative reactivity with a variety of substrates.[15–17] The detailed kinetic studies provide valuable mechanistic insight into the mechanism of the antioxidative reactions of 1: whether the reaction between 1 and oxyl radical species proceeds via one-step hydrogen atom transfer or via electron transfer.

Experimental Section

Materials. (+)-Catechin (1) was purchased from Sigma. Galvinoxyl radical (G•) was obtained commercially from Aldrich. $Mg(ClO_4)_2$ and acetonitrile (MeCN; spectral grade) were purchased from Nacalai Tesque, Inc., Japan, and used as received. Di-*tert*-butyl peroxide was obtained from Nacalai Tesque Co., Ltd., and purified by chromatography through alumina which removes traces of the hydroperoxide. Cumene was purchased from Wako Pure Chemical Ind. Ltd., Japan. Scandium trifluoromethanesulfonate, $Sc(OTf)_3$ ($OTf = OSO_2-CF_3$, 99%) was obtained from Pacific Metals Co., Ltd. (Taiheiyo Kinzoku). Propionitrile (EtCN) used as solvent was purified and dried by the standard procedure.[18]
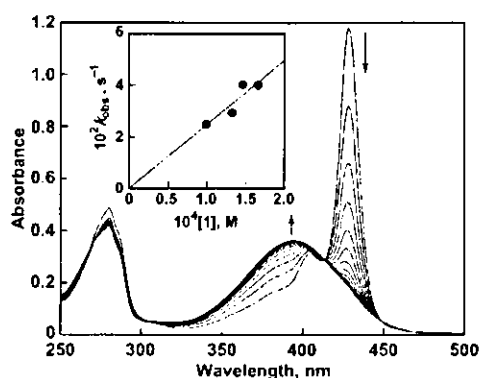
* Corresponding authors.
† National Institute of Radiological Sciences, Japan.
‡ National Institute of Health Sciences, Japan.
§ Shibaura Institute of Technology, Japan.
¹ Osaka University.

Figure 1. Spectral changes observed upon addition of 1 (1.5   10 ⁻¹ M) to a deaerated MeCN solution of G• (8.4   10 ⁻⁶ M) at 298 K (Interval: 10 s). Inset: plot of the pseudo-first-order rate constant (k_{obs}) vs the concentration of 1.

Spectral and Kinetic Measurements. Typically, an aliquot of (+)-catechin (1; 2.0 × 10 ⁻² M) in deaerated MeCN was added to a quartz cuvette (10 mm i.d.) which contained galvinoxyl radical (G•; 8.4 × 10⁻⁶ M) and Mg(ClO₄)₂ (0.1 M) in deaerated MeCN (3.0 mL). This led to a hydrogen-transfer reaction from 1 to G•. UV−vis spectral changes associated with this reaction were monitored using an Agilent 8453 photodiode array spectrophotometer. The rates of hydrogen transfer were determined by monitoring the absorbance change at 428 nm due to G• (ϵ = 1.43 × 10⁵ M⁻¹ cm⁻¹). Pseudo-first-order rate constants were determined by a least-squares curve fit using an Apple Macintosh personal computer. The first-order plots of ln(A − A∞) vs time (A and A∞ are denoted to the absorbance at the reaction time and the final absorbance, respectively) were linear until three or more half-lives with the correlation coefficient ρ > 0.999.

Kinetic measurements for the hydrogen-transfer reactions between 1 and cumylperoxyl radical were performed on a JEOL X-band spectrometer (JES-ME-LX) at 203 K. Typically, photoirradiation of an oxygen-saturated propionitrile (EtCN) solution containing di-tert-butyl peroxide (1.0 M) and cumene (1.0 M) with a 1000 W mercury lamp resulted in formation of cumylperoxyl radical (g = 2.0156), which could be detected at low temperatures. The g values were calibrated by using an Mn²⁺ marker. Upon cutting off the light, the decay of the ESR intensity was recorded with time. The decay rate was accelerated by the presence of 1 (1.0 × 10 ⁻⁴ M). Rates of hydrogen transfer from 1 to PhCMe₂OO• were monitored by measuring the decay of the ESR signal of PhCMe₂OO• in the presence of various concentrations of 1 in EtCN at 203 K. Pseudo-first-order rate constants were determined by a least-squares curve fit using a microcomputer. The first-order plots of ln(I − I∞) vs time (I and I∞ are the ESR intensity at time t and the final intensity, respectively) were linear for three or more half-lives with the correlation coefficient. ρ > 0.99. In each case, it was confirmed that the rate constants derived from at least five independent measurements agreed within an experimental error of ±5%.

Results and Discussion

Effect of Mg²⁺ on Hydrogen Transfer from (−)-Catechin to Galvinoxyl Radical. Upon addition of (+)-catechin (1) to a deaerated acetonitrile (MeCN) solution of galvinoxyl radical (G•), the absorption band at 428 nm due to G• disappeared immediately as shown in Figure 1. This indicates that hydrogen transfer from one of the OH groups on the B ring of 1 to G•
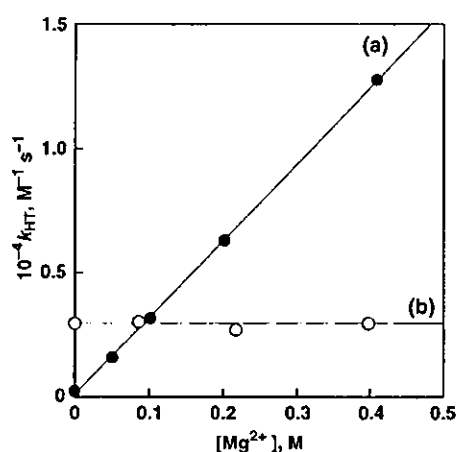
Figure 2. Plot of k_{HT} vs [Mg²⁺] in the hydrogen transfer from (a) 1 to G• and (b) 2 to G• in the presence of Mg(ClO₄)₂ in deaerated MeCN at 298 K.

takes place to give catechin radical (1•) and hydrogenated G• (GH) (eq 1).[19]
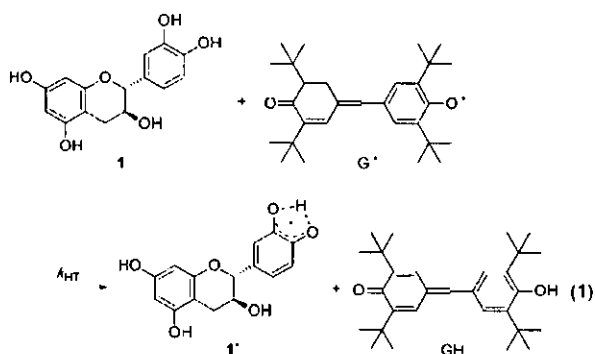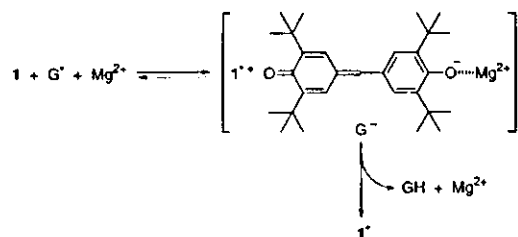

The decay of the absorbance at 428 nm due to G• obeyed pseudo-first-order kinetics when the concentration of 1 was maintained at more than 10-fold excess of the G• concentration. The observed pseudo-order-rate constant (k_{obs}) increases linearly with an increase in the concentration of 1 (inset of Figure 1). From the slope of the linear plot of k_{obs} vs the concentration of 1 is determined the second-order rate constant (k_{HT}) for the hydrogen transfer from 1 to G• at 298 K as 2.3 × 10² M⁻¹ s⁻¹. The 1• thus formed is known to be unstable and undergo disproportionation to produce the parent 1 and an o-quinone-type oxidized product of 1.[20]
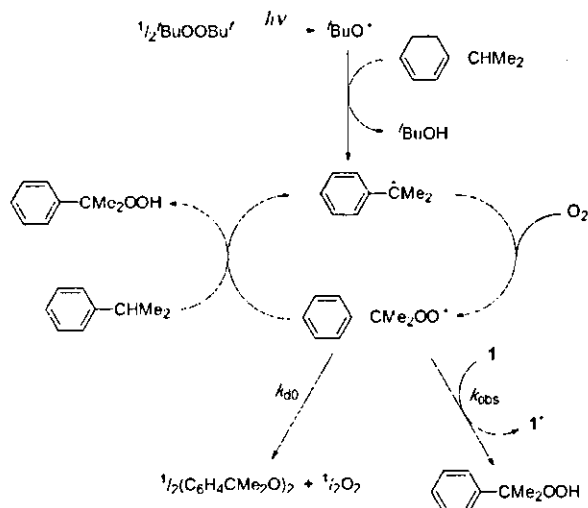
If the hydrogen transfer from 1 to G• involves an electron-transfer process as the rate-determining step, the rate of hydrogen transfer would be accelerated by the presence of magnesium ion.[14] This is checked by examining an effect of Mg²⁺ on the hydrogen transfer rate from 1 to G•. When Mg(ClO₄)₂ is added to the 1−G• system, the rate of hydrogen transfer from 1 to G• was significantly accelerated. The k_{HT} value increases linearly with increasing Mg²⁺ ion concentration as shown in Figure 2a (black circles). Thus, the hydrogen transfer may proceed via electron transfer from 1 to G•, which is accelerated by the presence of Mg²⁺, followed by proton transfer from 1•⁺ to G to yield 1• and GH as shown in Scheme 1. In such a case, the coordination of Mg²⁺ to the one-electron reduced species of G• (G⁻) may stabilize the product, resulting in the acceleration of electron transfer.

Hydrogen Transfer from (+)-Catechin to Cumylperoxyl Radical. Direct measurements of the rates of hydrogen transfer
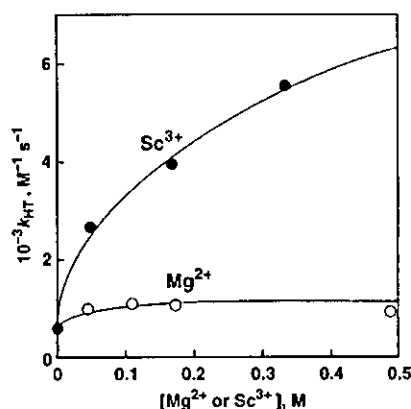
SCHEME 1

SCHEME 2

Figure 3. Plot of k_{HT} vs $[Mg^{2+}]$ (white circles) and $[Sc^{3+}]$ (black circles) in the hydrogen transfer from 1 to cumylperoxyl radical in the presence of $Mg(ClO_4)_2$ or $Sc(OTf)_3$ in EtCN at 203 K.

SCHEME 3

from (+)-catechin (1) to cumylperoxyl radical were performed in propionitrile (EtCN) at 203 K by means of ESR. The photoirradiation of an oxygen saturated EtCN solution containing di-*tert*-butylperoxide and cumene with a 1000 W mercury lamp results in formation of cumylperoxyl radical, which was readily detected by ESR. The cumylperoxyl radical is formed via a radical chain process shown in Scheme 2.[21][25] The photoirradiation of Bu^tOOBu^t results in the homolytic cleavage of the O—O bond to produce $Bu^tO^{•}$,[26,27] which abstracts a hydrogen from cumene to give cumyl radical, followed by the facile addition of oxygen to cumyl radical. The cumylperoxyl radical can also abstract a hydrogen atom from cumene in the propagation step to yield cumene hydroperoxide, accompanied by regeneration of cumyl radical (Scheme 2).[28,29] In the termination step, cumylperoxyl radicals decay by a bimolecular reaction to yield the corresponding peroxide and oxygen (Scheme 2).[28,29] When the light is cut off, the ESR signal intensity decays, obeying second-order kinetics due to the bimolecular reaction in Scheme 2.

In the presence of 1, the decay rate of cumylperoxyl radical after cutting off the light becomes much faster than that in the absence of 1. The decay rate in the presence of 1 (1.0×10^{-4} M) obeys pseudo-first-order kinetics. This decay process is ascribed to the hydrogen transfer from 1 to cumylperoxyl radical (Scheme 2). The pseudo-first-order rate constants increase with increasing 1 concentration to exhibit first-order dependence on [1]. From the slope of the linear plot of k_{obs} vs the concentration of 1 is determined the second-order rate constant (k_{HT}) for the hydrogen transfer from 1 to cumylperoxyl radical as 6.0×10^2 M^{-1} s^{-1} in EtCN at 203 K.

Mg^{2+} shows little acceleration effect on the rate of hydrogen transfer from 1 to cumylperoxyl radical as shown in Figure 3.
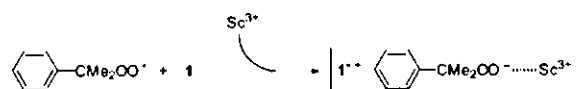
In contrast to the case of Mg^{2+}, the rate of hydrogen transfer from 1 to cumylperoxyl radical is enhanced significantly by the presence of $Sc(OTf)_3$ (OTf = triflate). Scandium ion has recently been reported to be the most effective promoter among various metal ions in metal ion-promoted electron-transfer reactions.[10] The k_{HT} values increase with increasing the scandium ion concentration, as shown in Figure 3. The acceleration effect of Sc^{3+} can be ascribed to the strong binding of Sc^{3+} to $PhCMe_2OO^{•}$, which results in a decrease in the free energy of the electron transfer as shown in Scheme 3. Thus, the electron transfer from 1 to cumylperoxyl radical becomes energetically feasible in the presence of Sc^{3+}. It should be noted that there is no interaction between cumylperoxyl radical and Sc^{3+}, since the g value of cumylperoxyl radical in the presence of Sc^{3+} is the same as the value in its absence.

Direct Hydrogen Atom Transfer vs Electron Transfer. Judging from the one-electron oxidation potential of 1 (E^o_{ox} vs SCE = 0.12 V),[13] which is higher than the one-electron reduction potential of $G^{•}$ (E^o_{red} vs SCE = 0.05 V), the free energy change of electron transfer from 1 to $G^{•}$ is positive [ΔG^o_{et} (in eV) = $e(E^o_{ox} - E^o_{red}) > 0$, where e is the elementary charge], and thereby the electron-transfer step is endergonic. In such a case, the overall rate of hydrogen transfer (k_{HT}), which consists of electron-transfer and proton-transfer steps, would be slower than the initial electron-transfer rate (k_{et}). The maximum k_{et} value is evaluated from the ΔG^o_{et} value by eq 2, where it is assumed that the activation free energy ($\Delta G^{\ne}_{et}$) is equal to ΔG_{et} (no additional barrier is involved). Z is the frequency factor taken as 1×10^{11} M^{-1} s^{-1}, and k_B is the Boltzmann constant.[41]

$$k_{et} = Z \exp(-\Delta G^o_{et}/k_B T) \qquad (2)$$

Figure 4 shows a plot of log k_{HT} versus ΔG^o_{et} calculated by eq 2 (denoted by ET line). The k_{HT} value of the 1–$G^{•}$ system (black circle) is much smaller than the corresponding maximum k_{et} value. This indicates that the hydrogen transfer proceeds via electron transfer followed by proton transfer as shown in Scheme 1 rather than a direct one-step hydrogen atom transfer. The hydrogen transfer from the vitamin E model, 2,2,5,7,8-pentamethyl-6-chromanol (2), to $G^{•}$ (eq 3) is known to proceed via a